Luminescence quenching of Ru(bpy)$_3{}^{2+}$ by nitrophenols in silicate thin films

M. Hamity, A. Senz, H.E. Gsponer *

Departamento de Química, Facultad de Ciencias Exactas, Fisicoquímicas y Naturales, Universidad Nacional de Río Cuarto, Ruta 36 Km 601, 5800 Río Cuarto, Argentina

Abstract

The luminescence quenching of ruthenium(II)–tris-1,2-bipyridine ion (Ru(bpy)$_3{}^{2+}$) included in methyltriethoxysilane-derived films by 2-, 3- and 4-nitrophenol was investigated. Sol–gel technology was used to prepare the "sol". Coating thin films were obtained from the "sol" by spin-coating on glass slide. A blue shift in the Ru(bpy)$_3{}^{2+}$ emission spectrum included in the films with respect to the aqueous solution was observed. Ru(bpy)$_3{}^{2+}$ luminescence quenching experiments were carried out with the quencher in aerated aqueous solution at pH 2 in contact with the film. The quenching plots obtained from either steady-state or time-resolved luminescence intensity measurements showed a downward curvature. Both plots were fitted satisfactorily by a sum of two terms of Stern–Volmer with quenching constants K_{SV1} and K_{SV2} associated to two different binding sites of the ruthenium complex, which indicates the presence of a matrix microheterogeneity in the films. The K_{SV1} and K_{SV2} values and the corresponding fractions of the total emission f_1^0 and f_2^0 for both sites suggest that only a low percentage of the probe is accessible to the quencher and that the probe is efficiently quenched in one of the sites, assigned to site 1. The value of its respective constant K_{SV1} was higher than the value of the constant K_{SV} in homogeneous aqueous solution. A dynamic process of electron transfer was suggested for the luminescence quenching of Ru(bpy)$_3{}^{2+}$ in the film by nitrophenols in aqueous solution.
© 2005 Published by Elsevier B.V.

Keywords: Thin films; Tris(2,2′-bipyridine)ruthenium(II); Luminescence; Quenching; Nitrophenol

1. Introduction

The photochemistry and photophysics of α-diimine–metal complexes, particularly tris(2,2′-bipyridine)ruthenium(II), Ru(bpy)$_3{}^{2+}$, have received much attention in the literature due to their unique properties, particularly strong luminescence, moderate excited state lifetime, appreciable reactivity of the excited state in electron and energy transfer reactions and relatively high thermal and chemical stability [1]. The luminescent excited state of Ru(bpy)$_3{}^{2+}$ is assigned to a metal-to-ligand charge-transfer (MLCT) state. Therefore, the luminescent properties of this complex are very sensitive to the polarity and viscosity of the environment. The dynamic properties of the MLCT state of Ru(bpy)$_3{}^{2+}$ and related complexes adsorbed on semiconductors have been widely studied [2–4]. There are also an important number of studies on Ru(bpy)$_3{}^{2+}$ adsorbed

on non-conducting materials such as SiO$_2$, which can actually modify photochemical reactions [5–9]. One of the current methods to prepare these materials has been the use of a low-temperature sol–gel-technology, route wherein a metal alkoxide precursor undergoes hydrolysis and condensation reactions to form a highly cross-linked solid [10]. The use of low temperatures allows the incorporation of a variety of dopants including organic, organometallic and biological molecules [11].

Phenolic compounds are one of the main contaminants of industrial waste [12]. In our laboratory, there is an increasing interest in the study of electron transfer reactions involving excited states of Ru(bpy)$_3{}^{2+}$ and tris-1,10-phenanthroline chromium(III) with phenolic derivatives in homogeneous as well as in microheterogeneous media [13–19]. The luminescence of Ru(bpy)$_3{}^{2+}$ has been used to determine the location of the complex in surfactant aggregates in solution and in the adsorbed state on solids, as in hemimicelles, as well as to study interactions between Ru(bpy)$_3{}^{2+}$ and the surface of solids [16,19–21]. More recently, we have studied the luminescence

_____

* Corresponding author. Tel.: +54 358 4676233; fax: +54 358 4676233.
  E-mail address: Hgsponer@exa.unrc.edu.ar (H.E. Gsponer).

decay, the spectral behaviour and the luminescence quenching of $Ru(bpy)_3^{2+}$ by 2,6-dimethylphenol and 4-bromo-2,6-dimethylphenol in sol–gel-processed silicate thin films [22,23]. We obtained a bimodal distribution of probe sites in the films from modeling of the emission decays. The luminescence quenching plots were fitted satisfactorily by a Stern–Volmer expression sum of two terms with quenching constants K_{SV1} and K_{SV2}, which can be associated to two different binding sites of the ruthenium complex.

However, to our knowledge, the luminescent properties of $Ru(bpy)_3^{2+}$ in silicate films in presence of nitrophenols in aqueous solution have not been studied yet. We report here a study on the luminescence of the MLCT state of $Ru(bpy)_3^{2+}$ included in the film quenched by 2-, 3-, and 4-NO_2PhOH in their neutral forms dissolved in an aqueous solution in contact with the film. Sol–gel technology was used to prepare the silicate thin films and the precursor was methyltrimethoxysilane (MTMOS). The results are discussed in terms of a bimodal distribution of probe sites in the films.

2. Experimental

2-NO_2PhOH, 3-NO_2PhOH and 4-NO_2PhOH (Aldrich) were purified by vacuum sublimation. Tris(2,2′-bipyridine) ruthenium(II) dichloride hexahydrate (Sigma) and $CH_3Si(OCH_3)_3$ (MTMOS) (Aldrich, 98%) were used as received. Chlorhidric acid (Cicarelli p.a.) and methanol (Merck p.a.) were used without further purification. Aqueous solutions were prepared with water purified by reverse osmosis, followed by ion exchange and activated charcoal (its typical conductivity was $18\,M\Omega^{-1}$).

2.1. "Sol" preparation

Methanol (MeOH) was used as co-solvent. The preparation with MTMOS was made at pH 4 and the following molar ratio MTMOS:H_2O:MeOH = 1:2:2. The mixture was then stirred for 24 h at 65 °C. The $Ru(bpy)_3^{2+}$ concentration in the precursor solution was 2×10^{-3} M.

2.2. Film processing

The glass slides were pretreated by soaking them in 1 M HCl (aq.) for 1 h, rinsing them with copious amounts of water and drying in an oven at 150 °C. The glass slides were cut to fit the diagonal length of a standard square cell fluorescence.

Coating films were prepared from the "sol" by spin-coating on a cleaned glass slide substrate at a speed of 4000 rpm during 60 s. The spin-coating of films was carried out with a rotatory Spin-Coater P-6 000 system. The films were then dried in an oven for 16 h at 70 °C.

2.3. Measurements

The quenching experiments with nitrophenols were carried out by using static and dynamic measurements. The steady-state luminescence intensity measurements were performed using a Spex Fluoromax DM3000 spectrofluorometer. The measurements of time-resolved luminescence intensity decay were carried out in a single photon-counting FL900DCT fluorescence spectrophotometer from Edinburgh Analytical Instruments.

Excitation was accomplished at 450 nm. Due to interference from the excitation source, the sample was placed in the fluorescence cell so that the light scattered or reflected by the film coming from the excitation beam diminished at the entrance of the detector. The excitation radiation was impinged on the film-coated side of the glass substrates at an incidence angle of 45° with a 90° angle maintained between the excitation beam trajectory and the emission collection optics. The emission intensities were recorded at the wavelength maximum of the non-corrected spectra. These intensities were calculated as relative values to a baseline obtained by extrapolation of the experimental data between 500 and 850 nm. We used this procedure, since it was not possible to prepare two identical films with and without $Ru(bpy)_3^{2+}$ and to perform a blank to correct the data by baseline.

The luminescence measurements were carried out in air-equilibrated aqueous solutions and the temperature was kept at 25 °C in the cell compartment with a water circulation thermostat.

For both measurement techniques, the solution in contact with the film was 0.01 M in HCl. At this HCl concentration, the pH is lower than the pK_a of the NO_2PhOH and thus its protonated form predominates in the acid–base equilibrium. The pK_a values are 7.22, 8.30 and 7.16 for 2-, 3- and 4-NO_2PhOH, respectively [24].

The experiments were carried out with at least six different quencher concentrations. The concentration of the phenolic compounds ranged from 2×10^{-4} to 4×10^{-3} M. In a typical experiment, 2 ml of an aqueous solution at pH 2 was added to the fluorescence cuvette containing the film, and successive aliquots of a concentrated NO_2PhOH stock solution were added using a Hamilton microliter syringe.

3. Results and discussion

3.1. Luminescence spectra

Fig. 1 shows the $Ru(bpy)_3^{2+}$ emission spectra for an MTMOS-derived film prepared from the "sol" with a molar ratio water:precursor (R_w) = 2:1 and spin-coated at 4000 rpm, in the presence and absence of 2-NO_2PhOH. The increase of the baseline when the wavelength decreases may be due to the light scattering produced by the glass substrate-film. However, as we could not perform a blank to correct the scattering, the correction in the luminescence intensity measurements at the emission spectrum was carried out from a baseline obtained by extrapolation of the experimental data (see Section 2 and Fig. 1).

Fig. 1 shows that the emission spectrum reached a maximum at 596 nm. On the other hand, in aqueous solution we obtained the non-corrected emission spectrum, which shows a band with a maximum at 609 nm. Then, the $Ru(bpy)_3^{2+}$ emission maximum was shifted to the blue in the MTMOS-derived film with respect
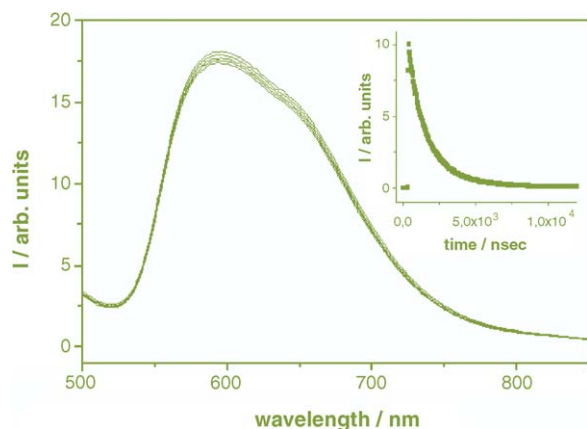
Fig. 1. Emission spectra of Ru(bpy)$_3{}^{2+}$ in spin-coated thin films of MTMOS in the presence of 2-NO$_2$PhOH in concentrations ranging from 0 to 4×10^{-3} M in aqueous solution at pH 2. *Inset*: Luminescence decay profile of Ru(bpy)$_3{}^{2+}$ in spin-coated thin films of MTMOS, in the absence of 2-NO$_2$PhOH, in aqueous solution at pH 2 and fitted by a double-exponential curve. Complete details are given in Sections 2.1 and 2.2.

to the aqueous solution. However, no changes were observed in the excitation spectrum.

These data can be explained in terms of excited state–environment interactions. The luminescent excited state of the Ru(II) complexes is assigned to the metal-to-ligand charge-transfer state (MLCT). When the complex is excited the solvent reorientation stabilizes the MLCT state, which has a large dipole moment. In the organically modified silicate thin films, the solvent molecules surrounding the Ru(bpy)$_3{}^{2+}$ complex are not fully free to move or rotate because of their possible interaction with the silanol groups (Si–OH) of the gel network. This restriction in the freedom of movement of the solvent molecules would cause the rigidochromism [25] of the Ru(bpy)$_3{}^{2+}$ complex. The excited state is not completely stabilized or relaxed within its lifetime, and hence, the emission occurs from a higher energy level than that in a fluid solution.

Similar spectroscopic results were obtained in our previous studies with films derived from MTMOS, methyltriethoxysilane (MTEOS), ethyltriethoxysilane (ETEOS) and tetraethoxysilane (TEOS) prepared by dip-coating or spin-coating [22,23]. This blue shift on the emission spectra of Ru(bpy)$_3{}^{2+}$ was also reported and discussed in detail by other authors for Ru(II) complexes in sol–gel materials [8,9,26,27].

3.2. Luminescence lifetimes

Emission decay profiles of the luminescent probe are even more sensitive to the microenvironment since they provide information on both the polarity of the surroundings (from the emission lifetime) and the distribution of binding sites within the material (multiexponential decays). Therefore, we carried out measurements of time-resolved luminescence intensity decays to obtain the excited state lifetimes of Ru(bpy)$_3{}^{2+}$ included in the film. The film was in contact with an aerated aqueous solution with or without addition of quencher stock solution. A typical decay curve is given in Fig. 1.

In previous studies [22,23], we observed that the luminescence decay of Ru(bpy)$_3{}^{2+}$ in organically modified silicate gel matrixes exhibited complex kinetics which cannot be modeled by a single exponential function. The luminescence decay profile was properly fitted by a bimodal distribution of rates (lifetimes, $\tau_{short} = \tau_1$ and $\tau_{long} = \tau_2$). Both rates can be attributed to the decay of the photo-excited ruthenium complex in two different binding sites, $m = 2$ in the Eq. (1):

$$I(t) = \sum_{i=1}^{m} \alpha_i e^{-t/\tau_i} \tag{1}$$

where α_i is the pre-exponential amplitude associated with the site i within the host matrix and τ_i is the corresponding excited state luminescence lifetime. This heterogeneity at the molecular level in this type of materials has been also reported by other authors [28–30].

The decay curve in Fig. 1, as all the luminescence decay data obtained in this work, supports this picture. Therefore, a value of $m = 2$ was used to fit the curves of luminescence intensity decays using the Eq. (1) in the absence or the presence of NO$_2$PhOH in the aqueous solution in contact with the film.

With the values obtained of the parameters τ_i and α_i, we calculated the pre-exponential weighted mean lifetime (τ_M) according to the Eq. (2):

$$\tau_M = \frac{\sum\limits_{i=1}^{2}(\alpha_i \tau_i)}{\sum\limits_{i=1}^{2}\alpha_i} \tag{2}$$

It is important to note that in this form of calculation of τ_M, the pre-exponential factors are normalized and therefore, the average lifetime obtained by Eq. (2) takes into account only the effect of the dynamic processes on the luminescence intensity decay.

3.3. Luminescence quenching

It can be observed in Fig. 1 that the emission spectrum of Ru(bpy)$_3{}^{2+}$ in the film was not qualitatively affected by the presence of 2-NO$_2$PhOH in the aqueous solution in contact with the film. The presence of the phenolic compound only produced a decrease in the luminescence intensity. From the data in Fig. 1, we obtained Stern–Volmer plots of I^0/I versus $[Q]$ which showed a downward curvature, as can be seen in Fig. 2. $[Q]$ is the molar concentration of the quencher dissolved in aqueous solution in contact with the film, and I^0 and I are the steady-state luminescence intensities in the absence and presence of the quencher, respectively.

Similar quenching plots were obtained in previous studies for other phenolic quenchers with MTEOS, MTMOS, ETEOS and TEOS-derived films [22,23]. This non-linearity of the plot has been frequently observed in Stern–Volmer plots for quenching of species in microheterogeneous media [31–33].

The analysis of the luminescence quenching results was based on a multisite model. The total luminescence emitted by the
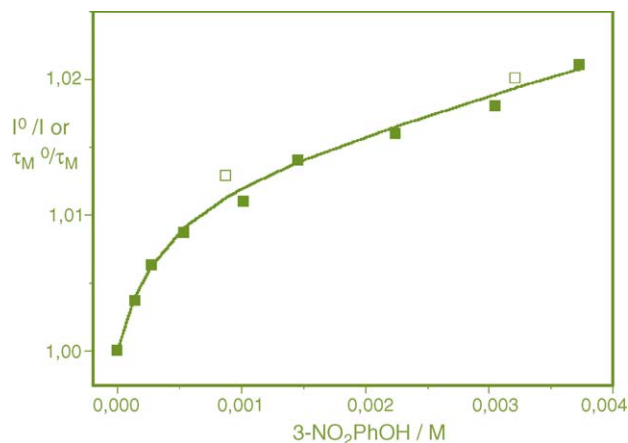
Fig. 2. Stern–Volmer plot for the luminescence quenching of $Ru(bpy)_3^{2+}$ in spin-coated thin films of MTMOS by $3-NO_2PhOH$ in aqueous solution at pH 2 and fitting of the data by Eq. [6]. Complete details are given in Sections 2.1 and 2.2. (■) τ_M^0/τ_M data; (□) I^0/I data.

Table 1
Luminescence quenching of the MLCT excited state of $Ru(bpy)_3^{2+}$ by NO_2PhOHs in water and in MTMOS-derived films at pH 2 (Stern–Volmer parameters, fitting of the data by Eq. (6), f_1^0 and K_{SVi} at $25 \pm 1\,°C$)

$Ru(bpy)_3^{2+}$ [a]	Quencher	K_{SV1} [b]	f_1^0 [b]	K_{SV2} [b]	f_2^0 [b]
In water	$2-NO_2PhOH$	1440[c]			
In water	$3-NO_2PhOH$	1840[c]			
In water	$4-NO_2PhOH$	1760[c]			
MTMOS[d]	$2-NO_2PhOH$	3010	0.014	5.2	0.986
		3920[e]	0.026[e]	11.3[e]	0.974[e]
MTMOS[d]	$3-NO_2PhOH$	3190	0.015	1.9	0.985
		3360[e]	0.011[e]	2.7[e]	0.989[e]
MTMOS[d]	$4-NO_2PhOH$	3260	0.007	1.1	0.993
		3160[e]	0.009[e]	1.0[e]	0.991[e]

[a] $Ru(bpy)_3^{2+}$ in water or in MTMOS-derived films.
[b] Estimated error ±20–30%.
[c] Ref. [17].
[d] Spin-coated thin films of MTMOS. Complete details are given in Sections 2.1 and 2.2.
[e] From steady-state luminescence intensity measurements.

probe, in the absence of the quencher, can be expressed as follows in terms of the luminescence quantum yield for the probe in the different sites:

$$\Phi_L^0 = \sum_{i=1}^{m} \Phi_{L_i}^0 \qquad (3)$$

and in the presence of quencher:

$$\Phi_L = \sum_{i=1}^{m} \Phi_{L_i} \qquad (4)$$

If the luminescence of the probe in whichever of the sites is independently quenched, it can be supposed that each one of them is quenched following a Stern–Volmer law:

$$\frac{\Phi_{L_i}^0}{\Phi_{L_i}} = f_i^0 \frac{\Phi_L^0}{\Phi_{L_i}} = 1 + K_{SVi}[Q] \qquad (5)$$

where the f_i^0 variable is the fraction of the total emission from the luminophore located at a site i under unquenched conditions and the K_{SVi} variable is the Stern–Volmer quenching constant associated to this site.

From the Eqs. (3)–(5) we obtain the overall quenching expression, which is simply the superposition of Stern–Volmer expressions, resulting in a summation over all sites given by:

$$\frac{\Phi_L^0}{\Phi_L} = \frac{\Phi_L^0}{\sum_{i=1}^{m} \Phi_{L_i}} = \left(\frac{\sum_{i=1}^{m} f_i^0}{1 + K_{SVi}[Q]} \right)^{-1} \qquad (6)$$

A good fitting of the steady-state luminescence intensity measurements was found by using Eq. (6) with $m = 2$ (see Fig. 2). Similar Stern–Volmer plots were obtained for $2-NO_2PhOH$ and $4-NO_2PhOH$. The Stern–Volmer quenching constants associated to each site, K_{SV1} and K_{SV2}, and the corresponding fractions of the total emission, f_1^0 and f_2^0, are shown in Table 1 for the nitrophenols used in this work.

On the other hand, from Eq. (2) the τ_M values were calculated in the absence and in the presence of quencher for various Q molar concentrations, τ_m^0 and τ_M respectively. The plot of τ_m^0/τ_m

versus $[Q]$ and the fitting of the data by Eq. (6) but applied to the mean lifetimes is also shown in Fig. 2. The Stern–Volmer quenching constants and fractions of the total emission associated to each site $K_{SV1} - f_1^0$ and $K_{SV2} - f_2^0$ obtained from lifetime measurements for the different nitrofenols studied are also shown in Table 1.

The experimental uncertainties in the steady-state luminescence intensity or luminescence decay measurements indicate that the error associated to the values of the Stern–Volmer parameters calculated from Eq. (6) are around 20–30%. Therefore, we may conclude that the K's and f^0's values obtained from both type of measurements are comparable.

The fraction of the total emission located at site 2 (f_2^0) ranged from 97.4 to 99.3%, and the K_{SV2} was 1.0–11.3 M^{-1} (Table 1). These results of f_2^0 and K_{SV2} indicate that a high percentage of the photo-excited $Ru(bpy)_3^{2+}$ is not accessible to the quencher and that the quenching process has a very low efficiency for this site within the host matrix in the films. This interpretation suggests that the probe in this site is placed either into a higher microviscosity microenvironment and/or in a location to which the quencher cannot access easily.

A different fraction of emission total not quenched dynamically by oxygen was found from the time-resolved luminescence intensity decay measurements for the film in aerated aqueous solutions. The fraction f_2^0 calculated as $\alpha_2 \times 100/(\alpha_1 + \alpha_2)$ was in the order of 30%. The parameters α_1 and α_2 are the pre-exponential factors of Eq. (1); the values used to calculate f_2^0 were obtained from the fitting of the luminescence decay profile shown in Fig. 1. Then, ~70% of the metallic complex within the film is accessible to oxygen molecules. This result is in agreement with the fact that most sol–gel-derived oxygen sensing applications inform 75–85% overall quenching response [34,30,22].

Therefore, from the above considerations, we can conclude that the luminescent species with long lifetime (τ_2) was comparatively less accessible to the nitrophenolic compounds studied

in this work than to oxygen molecules. It is well known that the molecular oxygen has several primary advantages in the quenching process such as its high collisional quenching efficiency and its high diffusion coefficient [35].

On the other hand, a low percentage of the probe at site 1 in the order of 0.7–2.6% was accessible to the quenchers NO_2PhOHs and efficiently quenched by them. The K_{SV1} values were in the range 3010–3920 M^{-1}.

Similar results were obtained in the study of dynamic electron transfer in aquo- and alco-SiO_2 gels using tetramethoxysilane as precursor [36]. Only the fast component (τ_1), which has a minor contribution to the decay, was dynamically quenched by methyl viologen adsorbed in $Ru(bpy)_3{}^{2+}$ doped aquogels. These quenching profiles are indicative of the matrix microheterogeneity in this type of materials and are fully consistent with the biexponential nature of the luminescence intensity decay profiles [28–30].

The values of the K_{SV1} constants given in Table 1 were higher than the ones of the K_{SV} constants corresponding to the luminescence quenching of $Ru(bpy)_3{}^{2+}$ by 2-, 3- and 4-NO_2PhOH in aqueous solution at pH 2 (ref. [17] and Table 1). A opposite tendency was found in the study of the luminescence quenching of $Ru(bpy)_3{}^{2+}$ included in films derived from MTMOS, MTEOS, ETEOS and TEOS by 2,6-dimethylphenol and 4-bromo-2,6-dimethylphenol [22,23]. In a first approach, it would seem that the highest quenching efficiency observed in this paper – high K_{SV1} values relative to K_{SV} values in aqueous solution – could be related to the different redox properties of the quenchers used in each case.

Now, we intend to make some considerations on the quenching mechanism. First, the Stern–Volmer parameters obtained from either steady-state luminescence intensity measurements or time-resolved luminescence intensity decay measurements are in good agreement within estimated error (±20–30%). Second, since τ_M calculated by using Eq. (2) takes into account only the dynamic quenching, the coincidence between the Stern–Volmer parameters from both measurements indicates that only this quenching process is operative (Fig. 2 and Table 1). Therefore, from these considerations, it would seem that the static quenching is not an important process in the quenching mechanism.

On the other hand, it is well known that groups that are considered classical meta directors (nitro, carbonyl, acetyl) make the phenol more difficult to oxidize by decreasing the electron density. The anodic half-wave potentials of 2-, 3- and 4-NO_2PhOH in aqueous solution indicate that the nitro-derived compounds should be easily reduced [37]. Thus, from this fact and the experimental results obtained in a previous study, we could assume that the quenching of the MLCT state of $Ru(bpy)_3{}^{2+}$ by nitrophenols takes place by an electron transfer mechanism in which the $Ru(bpy)_3{}^{2+}$ complex is oxidized in a dynamic process [17]. Therefore, we can consider that the $Ru(bpy)_3{}^{2+}$ luminescence quenching in the MTMOS-derived films by nitrophenols should be also a dynamic process of electron transfer.

In summary, a blue shift in the emission spectrum of the MLCT state of $Ru(bpy)_3{}^{2+}$ with respect to the aqueous solution was observed in the MTMOS-derived films. The excited state was not completely stabilized or relaxed within its lifetime. The luminescence decay profile was properly fitted by a bimodal distribution of rates. A luminescence quenching of the ruthenium complex in the films by 2-, 3- and 4-nitrophenol in aqueous solution at pH 2 was observed. The quenching plots obtained from either luminescence intensities or intensity decay measurements could be fitted satisfactorily by constants associated to two different binding sites of the ruthenium complex. This result is indicative of the matrix microheterogeneity in the films and is fully consistent with the biexponential nature of the luminescence intensity decay profiles. The Stern–Volmer quenching constants and fractions of the total emission associated to each site $K_{SV1} - f_1^0$ and $K_{SV2} - f_2^0$ were obtained. From the parameter values for both sites in the films it would seem that only a low percentage of the probe is accessible to the quencher. The Stern–Volmer constant values at the site 1, K_{SV1}, were higher than the K_{SV} values for $Ru(bpy)_3{}^{2+}$ in water for the same quenchers. We also postulated that the luminescence quenching of the MLCT state of $Ru(bpy)_3{}^{2+}$ in the MTMOS-derived films by nitrophenols in aqueous solution is a dynamic process of electron transfer.

Acknowledgment

References

[1] K. Kalyanasundaram, Photochemistry of Polypiridines and Porphyrin Complexes, Academic Press, London, 1992.
[2] J. Desilvestro, M. Gratzel, L. Kavan, J. Moser, J. Augustynski, J. Am. Chem. Soc. 107 (1985) 2988.
[3] B. O'Reagan, J. Moser, M. Anderson, M. Gratzel, J. Phys. Chem. 94 (1990) 8720.
[4] K. Hashimoto, M. Hiramoto, T. Kajiwara, T. Sakata, J. Phys. Chem. 92 (1988) 4636.
[5] J.K. Thomas, J. Wheeler, J. Photochem. 28 (1985) 285.
[6] P.V. Kamat, W.E. Ford, J. Phys. Chem. 93 (1989) 1405.
[7] J. Fan, W. Shi, S. Tysoe, T.C. Strekas, H.D. Gafney, J. Phys. Chem. 93 (1989) 373.
[8] K. Matsui, F. Momose, Chem. Mater. 9 (1997) 2588.
[9] P. Innocenzi, H. Kozuka, T. Yoko, J. Phys. Chem. B 101 (1997) 2285.
[10] L.L. Hench, J.K. West, Chem. Rev. 90 (1990) 33.
[11] D. Avnir, S. Braun, O. Lev, M. Ottolenghi, Chem. Mater. 6 (1994) 1605.
[12] M. Kuwahara, N. Shindo, K. Minakata, J. Agric. Chem. Soc. Jpn. 44 (1970) 169.
[13] D.M. Vera, G.A. Argüello, G.A. Argüello, H.E. Gsponer, J. Photochem. Photobiol. A: Chem. 76 (1993) 13.
[14] A. Senz, H.E. Gsponer, J. Colloid Interface Sci. 165 (1994) 60.
[15] A. Senz, H.E. Gsponer, J. Phys. Org. Chem. 8 (1995) 706.
[16] A. Senz, H.E. Gsponer, J. Colloid Interface Sci. 180 (1996) 193.
[17] A. Senz, H.E. Gsponer, J. Colloid Interface Sci. 195 (1997) 94.
[18] D. Pagliero, G.A. Argüello, H.E. Gsponer, J. Colloid Interface Sci. 215 (1999) 16.
[19] S. López, A. Senz, H.E. Gsponer, J. Colloid Interface Sci. 224 (2000) 126.
[20] D. Meisel, M.S. Matheson, J. Rabani, J. Am. Chem. Soc. 100 (1978) 117.
[21] J.T. Kunjappu, P. Somasundaran, N.J. Turro, J. Phys. Chem. 94 (1990) 8464.

[22] S. López, A. Senz, H.E. Gsponer, J. Colloid Interface Sci. 246 (2002) 122.

[23] M. Altamirano, A. Senz, H.E. Gsponer, J. Colloid Interface Sci. 270 (2004) 364.

[24] R.T. Morrison, R.N. Boyd, Organic Chemistry, Fondo Educativo Interamericano, México, 1985.

[25] S.J. Milder, J.S. Gold, D.S. Kliger, J. Phys. Chem. 90 (1986) 548.

[26] F.N. Castellano, T.A. Heimer, M.T. Tandhasetti, G.J. Meyer, Chem. Mater. 6 (1994) 1041.

[27] K. Matsui, K. Sasaki, N. Takahashi, Langmuir 7 (1991) 2866.

[28] U. Narang, J.D. Jordan, F.V. Bright, P.N. Prasad, J. Phys. Chem. 98 (1994) 8101.

[29] R.A. Dunbar, J.D. Jordan, F.V. Bright, Anal. Chem. 68 (1996) 604.

[30] G.A. Baker, B.R. Wenner, A.N. Watkins, F.V. Bright, J. Sol Gel Sci. Technol. 17 (2000) 71.

[31] E.R. Carraway, J.N. Demas, B.A. DeGraff, J.R. Bacon, Anal. Chem. 63 (1991) 337.

[32] A. Mills, M. Thomas, Analyst 122 (1997) 63.

[33] J.N. Demas, B.A. DeGraff, W. Xu, Anal. Chem. 67 (1995) 1377.

[34] A.K. McEvoy, C.M. McDonagh, B.D. MacCraith, Analyst 121 (1996) 785.

[35] J.R. Lakowicz, Principles of Fluorescence Spectroscopy, Plenum Press, New York, NY, 1992.

[36] F.N. Castellano, G.J. Meyer, J. Phys. Chem. 99 (1995) 14742.

[37] J.C. Suatoni, R.E. Snyder, R.O. Clark, Anal. Chem. 33 (1961) 1894.